Journal of Renewable Materials
DOI:10.32604/jrm.2020.011870
Article

Tech Science Press

3D Printing of Polylactic Acid Bioplastic–Carbon Fibres and Twisted Kevlar Composites Through Coextrusion Using Fused Deposition Modeling

J. Y. Tey*, W. H. Yeo, Y. J. King and W. O. Ding

Department of Mechanical and Material Engineering, Lee Kong Chian Faculty of Engineering and Science, Universiti Tunku Abdul Rahman, Jalan Sungai Long, Bandar Sungai Long, Cheras, 43000 Kajang, Selangor, Malaysia
*Corresponding Author: J. Y. Tey. Email: teyjy@utar.edu.my
Received: 02 June 2020; Accepted: 28 August 2020

Abstract: Polylactic acid (PLA) bioplastic is a common material used in Fused Deposition Modeling (FDM) 3D printing. It is biodegradable and environmentally friendly biopolymer which made out of corn. However, it exhibits weak mechanical properties which reduced its usability as a functional prototype in a real-world application. In the present study, two PLA composites are created through coextruded with 3K carbon fibres and twisted Kevlar string (as core fibre) to form a fibre reinforced parts (FRP). The mechanical strength of printed parts was examined using ASTM D638 standard with a strain rate of 1 mm/min. It has been demonstrated that the FRPs coextruded with 3K carbon fibres had achieved significant improvement in Young's modulus (+180.6%, 9.205 GPa), ultimate tensile strength (+175.3%, 103 MPa) and maximum tensile strain (+21.6%, 1.833%). Although the Young's modulus of Kevlar FRP was found to be similar to as compared to unreinforced PLA (~3.29 GPa), it has gained significant increment in terms of maximum tensile strain (+179.7%, 104.64 MPa), and maximum tensile strain (+257%, 5.384%). Thus, this study revealed two unique composite materials, in which the 3K carbon FRP can offer stiff and high strength structure while Kevlar FRP offers similar strength but at a higher elasticity.

Keywords: 3D printing; Kevlar fibre; 3K carbon fibre; coextruded reinforced plastic; polylactic acid bioplastic

1 Introduction

3D printing or additive manufacturing (AM) is a process that builds three-dimensional objects from bottom-up by layering material on the build plate. AM is capable of fabricating a variety of products with complex geometries that are often difficult to machine by using traditional manufacturing methods. In addition, it is also able to reduce resources consumption during the manufacturing process and recover the waste materials for recycling purposes [1]. Among the additive manufacturing technologies, fused deposition modelling (FDM) is the most popular and extensively studied by researchers. This is mainly because the method is relatively cheap and easier to construct and operate as compared to other processes which required control environments such as binder jetting or stereolithography [2]. In FDM, the thermoplastic filament is fed into a pinch roller mechanism to drive the filament into a heated block. Then

This work is licensed under a Creative Commons Attribution 4.0 International License, which permits unrestricted use, distribution, and reproduction in any medium, provided the original work is properly cited.

the melted filament will be extruded through a nozzle and print layer-by-layer to form the printed object. The printing process is slow, therefore compromise in resolution is required to gain a faster printing process.

Even though FDM seems to be promising in rapid prototyping and domestic use nowadays, but the printed part cannot perform as functional parts. This is mainly due to the thermoplastic printed parts (ABS, ASA, PC, PA 12, PC-ABS, PC-ISO, PPSF, ULTEM 9085, ULTEM1010 and etc.) are mechanically weak, their tensile strength are commonly in a range of 30 MPa to 72 MPa [2]. As the printed part is formed layer-by-layer, the material continuity only appears in direction inline with the printing motion. This is resulting the strength and stiffness of printed part are strongly depending on the Van der Waals bonding between layers and could weaken by the air gaps and voids that may form during the printing process [3]. Therefore, there is an urgent need to improve the strength of FDM products to unlock its possibility as a functional and load-bearing part [4,5].

CFRP is an alternative material to replace thermoplastic and metal due to its excellent mechanical strength. There have been a small number of reports on the 3D print of fibre reinforced polymer composites [6–11]. For example, Ferreira et al. [12] studied the mechanical characterization of 3D printed PLA and PLA reinforced with short carbon fibres. They incorporated 15 wt% of short carbon fibres and managed to obtain tensile modulus of 7.54 GPa and Tensile strength 53.4 MPa. This level of performance remains low as compared to continuous fibre reinforced plastic (CFRP) materials. Similar observation also reported in Blok et al. [13], whereby the authors observed that the strength and stiffness of the printed short fibre-reinforced composite can increase only by around 65%, which is considerably low. On the other hand, Li et al. [14] attained the tensile strength of continuous carbon-reinforced polylactic-acid (PLA) with 80–91 MPa as compared to 28 MPa in unmodified printed PLA samples. While Heidari-Rarani et al. [15] also reported the increased of tensile strength, which the continuous carbon-reinforced PLA achieved 61.4 MPa as compared to 45 MPa in pure PLA. The impressive improvement in mechanical strength of printed CFRP parts encouraged current research to further explore for others variant of continuous fibre such 3K carbon fibre and twisted Kevlar in the printed PLA.

This study aims to design and develop a CFRP co-extruder with 3K carbon fibre/ twisted Kevlar as core material and polylactic acid (PLA) as a matrix. Flow and thermal simulations were also involved to evaluate the performance of co-extruder. Besides, CFRP parts were printed and tested to investigate the influence of reinforced printed parts with 3K carbon fibre and twisted Kevlar towards the respective mechanical parts strength.

2 Materials and Methods

2.1 Materials

In this study, a twisted Kevlar thread (Dupont USA) and 3K carbon fibre (Toray Carbon Fibers America, Inc) (Fig. 1) were used to reinforced PLA matrix. Tab. 1 shows the mechanical properties of the fibre strings obtained from tensile test based on ASTM D3822 [16–18]. The respective stress-strain curves of both fibres are represented in Fig. 2. It is noticeable that 3K carbon fibre is having two times the breaking strength as compared to twisted Kevlar string. On the other hand, twisted Kevlar string has 3.33 times the strain elongation as compared to 3K carbon fibre string (Fig. 2). This is expected to lead to two distinctive mechanical characteristics on the printed FRP. The FRP was printed with a width of 2 mm and a height of 0.8 mm with both types of strings. The volume fraction of 3K carbon fibre and twisted Kevlar FRP were 1.96% and 7.85%, respectively.

On the other hand, PLA is a bioplastic where it exhibits low glass transition temperature and weak mechanical properties as indicated in Tab. 2. It behaves as a non-Newtonian fashion after glass transition temperature. In terms of its rheology behaviour, the viscosity curve of PLA at an extrusion temperature of 170°C can be fitted to the power-law model as presented in Eq. (1) [7].

Figure 1: Twisted Kevlar thread (left) and 3K Carbon Fibre (right)

Table 1: Technical data of Carbon Fibre and Twisted Kevlar based on experimental

Properties	3k Carbon Fibre	Twisted Kevlar
Breaking strength (MPa)	3211	1402
Tensile modulus (GPa)	212.3	26.677
Strain (%)	1.5	5
Linear density (tex)	198	167
Thread/yarn diameter (mm)	0.2	0.40

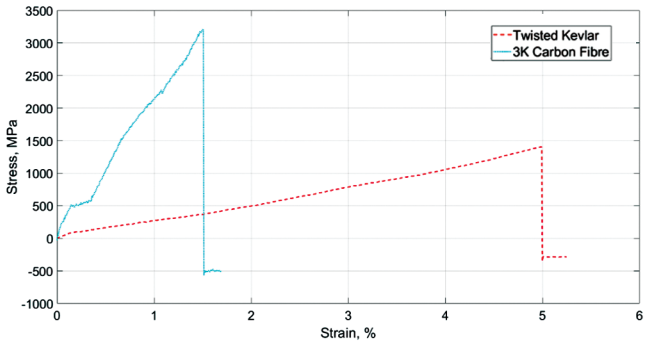

Figure 2: Tensile test against Twisted Kevlar and 3K Carbon Fibre

Table 2: Properties of PLA filament

Properties	PLA
Density, ρ (kg/m^3)	1260
Young's Modulus (GPa)	3.22
Poison's Ratio	0.3
Ultimate Tensile Strength (MPa)	37
Glass transition temperature, T_g (°C)	60
Melting temperature, T_m (°C)	145–160

$$\eta = 241721\gamma^{-0.7031} \quad (1)$$

where, η is viscosity (Pa.s) and γ is shear rate (s^{-1}).

2.2 Design of the Coextruder Hotend

A conventional desktop fused deposition method 3D printer was employed in the study. A simple modification was performed on the conventional hotend and the new design is shown in Fig. 3. A stainless-steel tube was inserted into the heat block of the hotend with the used of 2 mm nozzle. Due to the high viscosity of the melted PLA, the shear force generated can pull and drag the fibre towards the outlet of the nozzle. This is verified with flow simulation using ANSYS Fluent. In the computational fluid dynamic simulation, the PLA is model as a non-Newtonian fluid at the extruding temperature of 170°C with the use of the power-law model as stated in Eq. (1). The inlet velocity flow of the PLA is defined correlated to the printing speed of 150 mm/min. Two contours were plotted on the symmetry plane to show the pressure built up in the heated block and velocity of PLA flow at 170°C (Fig. 4). Maximum pressure of 33.6 kPa was observed at Ø3mm inlet. Therefore, the driving force of 0.24 N can be estimated as the required force by the extruder motor. This value is reasonable because the printing speed was relatively slow (150 mm/min). On the other hand, velocity contour shows an even flow of PLA at the outlet of the nozzle which enables the core fibre to be encapsulated into the PLA matrix. Shear force near the outlet of the nozzle was recorded between 852 kPa to 947 kPa, which was considered reasonably high to drag the fibre when printing. However, the only drawback of the design is that the fibre cannot be fully encapsulated within the PLA to formed an in-fibre cored structured. The fibre tends to stay at the top layer of the printed filament as indicated in Fig. 3. Nevertheless, this imperfection would not significantly affect the mechanical strength of the FRP as the encapsulation of the fibre could also be formed between the layers.

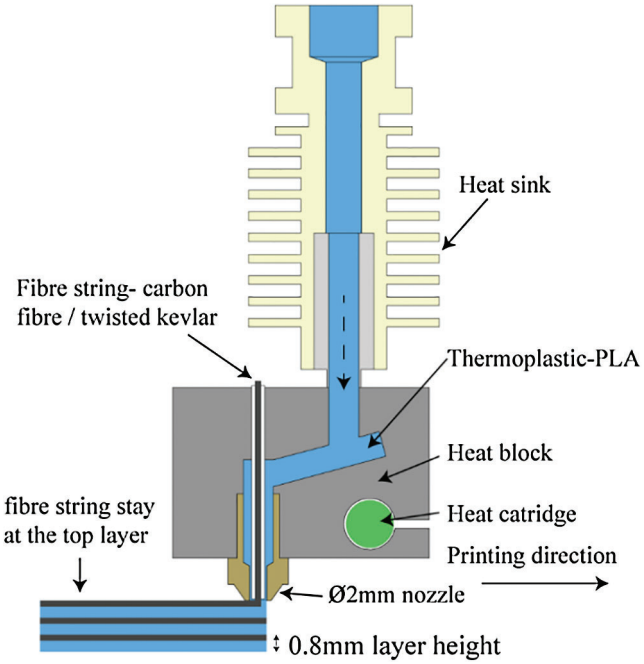

Figure 3: Design of co-extruder hotend

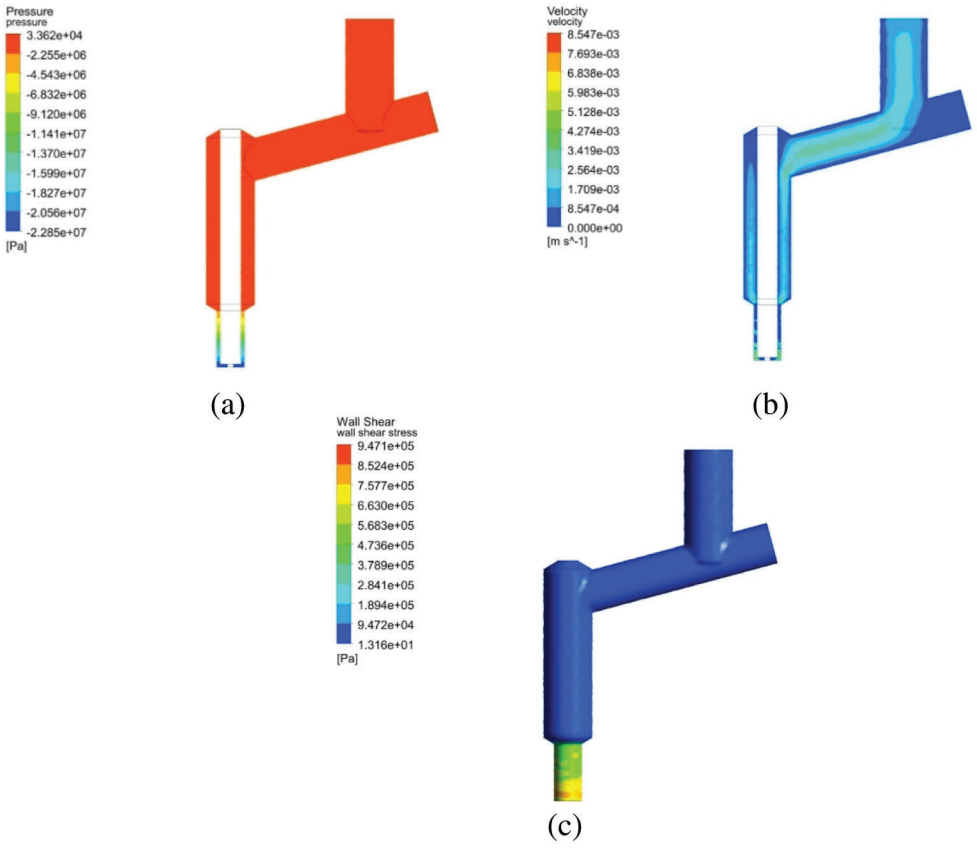

Figure 4: (a) Pressure contour, (b) velocity contour, and (c) Shear force contour at the wall

2.3 Experiment Procedures

The specimens were printed by referring to ASTM D638 standard to determine their mechanical strength with respect to their core reinforcement. These three groups are 3K carbon fibre reinforced PLA, Twisted Kevlar-reinforced PLA and plain PLA; each group consists of 3 specimens. An ASTM D638 Type I specimen as shown in Fig. 5 was employed in the tensile test. All FRP parts were printed with printing parameters as shown in Tab. 3. For non-reinforced specimens, a different set of printing parameters was used as a result of smaller nozzle size was employed due to the size of thermoplastic filament for printing was only 1.75 mm. The tensile test of each specimen was carried out at a strain rate of 1 mm/min.

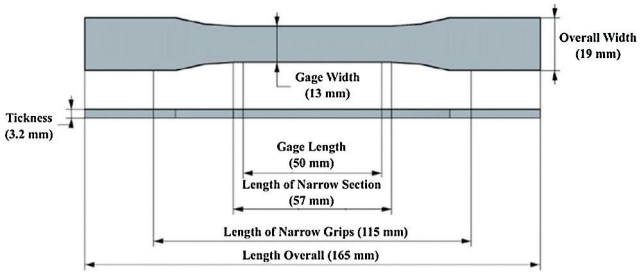

Figure 5: Dimension of ASTM D638 Type I specimen

Table 3: Printing parameters for specimens

Parameters	CFRP specimens	Non-reinforced specimen
Print speed (mm/min)	150	1000
Infill (%)	100	100
Infill pattern	Concentric	Concentric
Layer height (mm)	0.8	0.2
Nozzle size (mm)	2	0.4
Printing temperature (˚C)	175	190

3 Results and Discussion

Each FRP specimens consists of 4 layers; each layer was printed with 4 concentric patterns. Despite that co-extrusion was successful, a minor imperfection on the printed part due to the last layer of core fibre was exposed rather than encapsulated by PLA matrix (Fig. 6) as explained in Section 2.2.

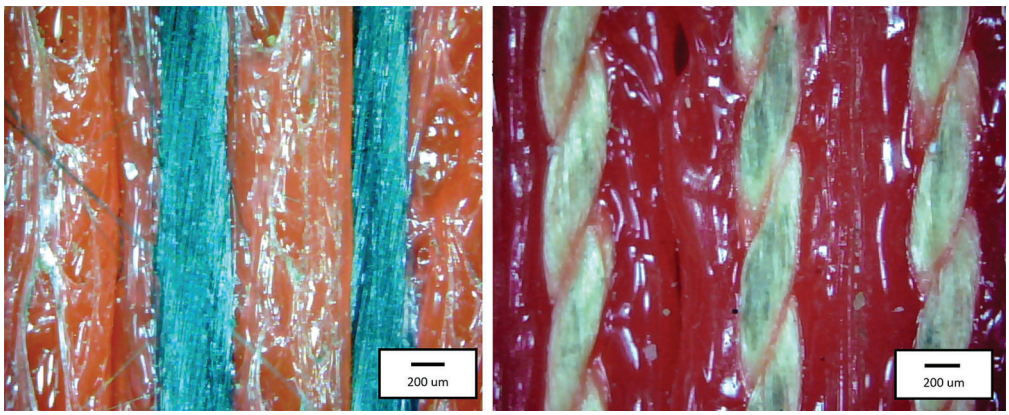

Figure 6: Microscope view of carbon fibre reinforced PLA (left) and Kevlar reinforced PLA (right)

All data in tensile tests were summarised in Tab. 4 and Fig. 7. First of all, 3K carbon fibre, FRP specimens were having average Young's modulus and ultimate tensile strength of 9.2 GPa and 103 MPa, respectively. This is equivalent to the respective improvement of 180.5% and 175.3% as compared to plain PLA specimens. As for maximum tensile strain, only marginal decrement of 18% was observed in 3K carbon fibre FRP. Given the volume fraction of 3K carbon fibre in printed FRP is only 1.96%, the mechanical strength of the 3D printed part had been greatly improved. On the other hand, twisted Kevlar FRP specimens were able to achieve an ultimate tensile strength of 104.64 MPa, Young's modulus of 3.29 GPa and a maximum strain of 5.65%. The equivalent improvement of each property as compared to plain PLA specimens was 179.7%, 0.3% and 152.7%, respectively. The relatively low tensile modulus and high maximum strain could be due to the twisting effect of Kevlar fibre. A high twist multiplier can increase the maximum elongation of Kevlar yarn while adversely affect the modulus of yarn [19]. Besides the improvement of strength, the addition of core fibre also alters the overall shape of the stress-strain curve of the specimen. Plain PLA parts went through a small amount of necking before fracture (Fig. 7). In contrast, both twisted Kevlar FRP and 3K carbon FRP were fractured immediately after the ultimate tensile stress (UTS) because necking is impossible with the addition of core fibre. Moreover, the stress-strain curve of carbon FRP parts has a slight decrease of Young's modulus before it reached the UTS, this could be due to the occurrence of matrix and fibre interface debonding as reported in the previous study [9].

Table 4: Tensile test result summary

Mechanical Properties	PLA	Twisted Kevlar-PLA	3K Carbon Fibre-PLA
Average Ultimate Tensile Strength (MPa)	37.41 ± 3.83	104.64 ± 1.27 (+179.7%)	103 ± 11.81 (+175.3%)
Average Breaking Strain (%)	2.236 ± 0.397	5.65 ± 3.2 (+152.7%)	1.833 ± 0.219 (−18%)
Average Elastic Modulus (GPa)	3.28 ± 0.18	3.29 ± 0.142 (0.3%)	9.2 ± 9.61 (180.5%)

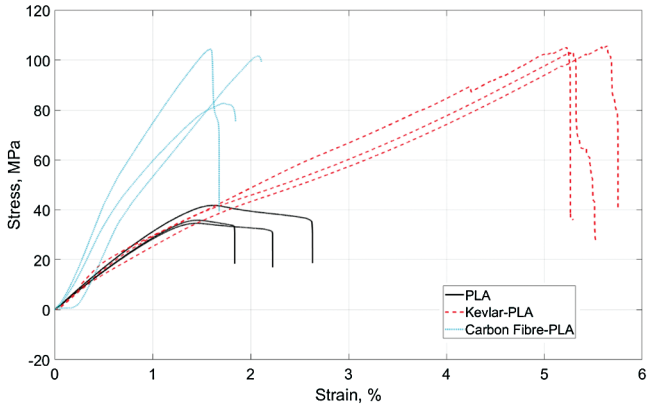

Figure 7: Tensile stress-strain curve

All plain PLA specimens were fractured within the gage length. However, all FRP specimens were broken near clamp location rather than at the middle gage length of the specimen as shown in Fig. 8. The cracks coincidentally happened with similar fashion whereby the started at the base PLA matrix. A similar observation was also reported in the literature of Dickson et al. [20]. These regions (shoulder of the dog bone) have the highest 3rd principal stresses (locations of highest compression). Therefore, failure in this region could be attributed to the shear forces experienced by the offset fibre alignment [20].

To further investigate this phenomenon, a finite element analysis (FEA) was carried out to verify the failure mode present in the test. A linear static analysis is modelled with the FRP specimen based on material properties obtained in Tabs. 1 and 2. The fibre core was modelled as a beam element and with bonded contact against the PLA matrix. A converged mesh size of 0.8 mm was applied to the model. The setup of the modelling was resembling the tensile test machine boundary condition whereby one side of the specimen was clamp (blue region—Fig. 9) and the remaining area was displaced (yellow region—Fig. 9) until ultimate strain rate found in the experimental result (Tab. 4).

The simulated Von misses stress result for both 3K carbon fibre FRP (Fig. 10) and twisted Kevlar FRP (Fig. 11) was plotted. It is noticeable that the stress was concentrated in the clamping location, where the cracking could start at the edge of the clamping side. This is mainly due to that the clamp area is lag of support by the in-core fibre as the Von misses stress of the string for both types of FRP was minimal as illustrated in Figs. 10b and 11b.

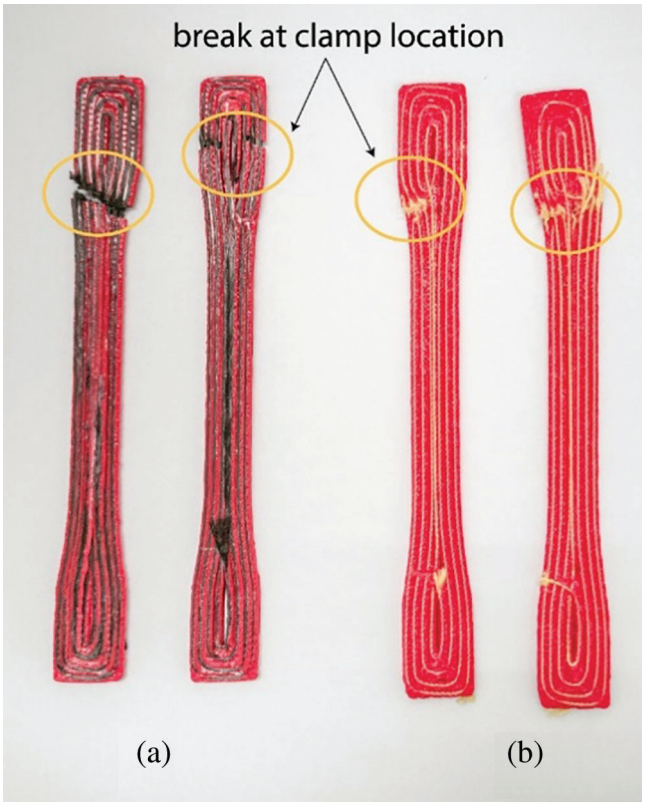

Figure 8: (a) Carbon fibre reinforced parts (left), (b) Kevlar reinforced parts

Figure 9: Specimen modelling boundary condition

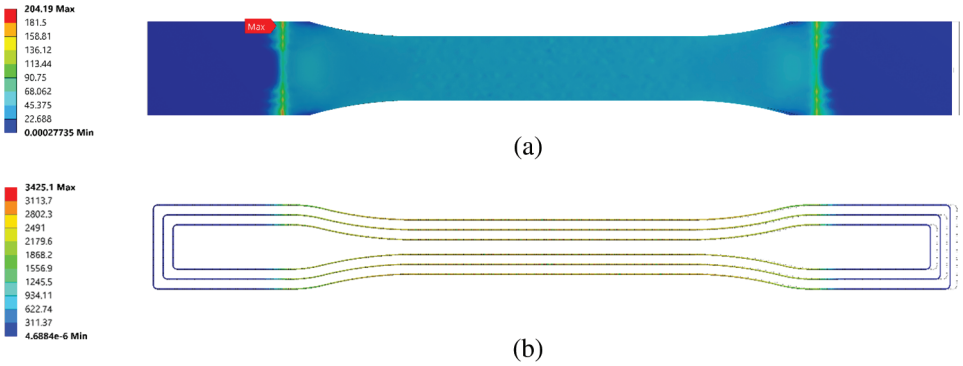

Figure 10: FEA result of Von misses Stress of (a) PLA matrix and (b) 3K Carbon Fibre

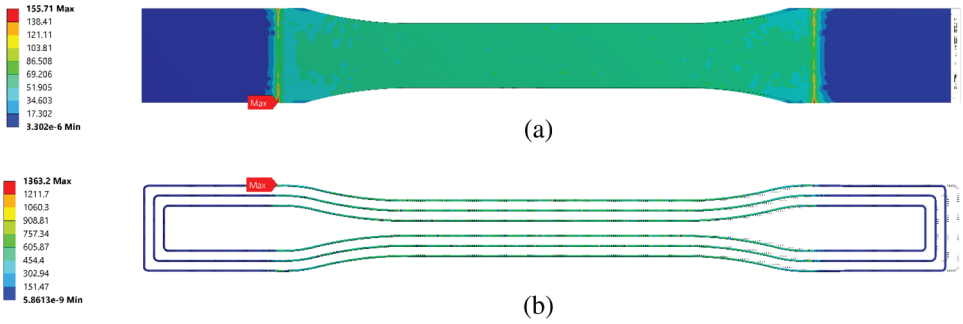

Figure 11: FEA result of Von misses Stress of (a) PLA matrix and (b) Twisted Kevlar

4 Conclusion

In this study, continuous fibre reinforced composite parts were produced by using FDM 3D printer with a customized co-extruder hotend. The core fibre and thermoplastic filament were extruded simultaneously to form the new composite material. Two new composites were printed in present work i.e., 3K carbon fibre reinforced PLA and twisted Kevlar-reinforced PLA composite. Both composites were found to exhibit improvement of tensile strength as compared to pure PLA printed part. Furthermore, with only 1.96% volume fraction of 3K carbon fibre, the composite mechanical strength could reach +175.3% in ultimate tensile strength and +180.5% in Young modulus. On the other hand, with a volume fraction of 7.85% for twisted Kevlar FRP, the composite could achieve improvement of +179.7% in ultimate tensile strength of PLA parts. Nevertheless, the minor drawback was observed such as breaking without necking. Overall, the proposed method provides an alternative way of fabricating composite materials, this promising technology shall be further explored to overcome the drawback of the method and improve the finishing of the printed parts.

Funding Statement: This project is funded by Universiti Tunku Abdul Rahman through the grant number IPSR/RMC/UTARRF/2018-C2/T02.

Conflicts of Interest: The authors declare that they have no conflicts of interest to report regarding the present study.

References

1. Ford, S., Despeisse, M. (2016). Additive manufacturing and sustainability: An exploratory study of the advantages and challenges. *Journal of Cleaner Production, 137,* 1573–1587. DOI 10.1016/j.jclepro.2016.04.150.
2. Calignano, F., Manfredi, D., Ambrosio, E. P., Biamino, S., Lombardi, M. et al. (2017). Overview on additive manufacturing technologies. *Proceedings of the IEEE, 105(4),* 593–612. DOI 10.1109/JPROC.2016.2625098.
3. Brian, N. T., Strong, R., Scott, A. G. (2014). A review of melt extrusion additive manufacturing processes: I. Process design and modeling. *Rapid Prototyping Journal, 20(3),* 192–204. DOI 10.1108/RPJ-01-2013-0012.
4. Parandoush, P., Lin, D. (2017). A review on additive manufacturing of polymer-fiber composites. *Composite Structures, 182,* 36–53. DOI 10.1016/j.compstruct.2017.08.088.
5. Al-Saleh, M. H., Sundararaj, U. (2011). Review of the mechanical properties of carbon nanofiber/polymer composites. *Composites Part A: Applied Science and Manufacturing, 42(12),* 2126–2142. DOI 10.1016/j.compositesa.2011.08.005.
6. Tey, J. Y., Ding, W. O., Yeo, W. H., King, Y. J., Saw, L. H. (2020). 3D printing of continuous kevlar reinforced polymer composite through coextrusion method. *IOP Conference Series: Earth and Environmental Science, 463,* 012091. DOI 10.1088/1755-1315/463/1/012091.
7. Quan, Z., Wu, A., Keefe, M., Qin, X., Yu, J. et al. (2015). Additive manufacturing of multi-directional preforms for composites: opportunities and challenges. *Materials Today, 18(9),* 503–512. DOI 10.1016/j.mattod.2015.05.001.

8. Caminero, M. A., Chacón, J. M., García-Moreno, I., Rodríguez, G. P. (2018). Impact damage resistance of 3D printed continuous fibre reinforced thermoplastic composites using fused deposition modelling. *Composites Part B: Engineering, 148,* 93–103. DOI 10.1016/j.compositesb.2018.04.054.
9. Zhang, H., Yang, D., Sheng, Y. (2018). Performance-driven 3D printing of continuous curved carbon fibre reinforced polymer composites: A preliminary numerical study. *Composites Part B: Engineering, 151,* 256–264. DOI 10.1016/j.compositesb.2018.06.017.
10. Der Klift, F. V., Koga, Y., Todoroki, A., Ueda, M., Hirano, Y. et al. (2016). 3D printing of continuous carbon fibre reinforced thermo-plastic (CFRTP) tensile test specimens. *Open Journal of Composite Materials, 6(1),* 18–27. DOI 10.4236/ojcm.2016.61003.
11. Matsuzaki, R., Ueda, M., Namiki, M., Jeong, T. K., Asahara, H. et al. (2016). Three-dimensional printing of continuous-fiber composites by in-nozzle impregnation. *Scientific Reports, 6(1),* 23058. DOI 10.1038/srep23058.
12. Ferreira, R. T. L., Amatte, I. C., Dutra, T. A., Bürger, D. (2017). Experimental characterization and micrography of 3D printed PLA and PLA reinforced with short carbon fibers. *Composites Part B: Engineering, 124,* 88–100. DOI 10.1016/j.compositesb.2017.05.013.
13. Blok, L. G., Longana, M. L., Yu, H., Woods, B. K. S. (2018). An investigation into 3D printing of fibre reinforced thermoplastic composites. *Additive Manufacturing, 22,* 176–186. DOI 10.1016/j.addma.2018.04.039.
14. Li, N., Li, Y., Liu, S. (2016). Rapid prototyping of continuous carbon fiber reinforced polylactic acid composites by 3D printing. *Journal of Materials Processing Technology, 238,* 218–225. DOI 10.1016/j.jmatprotec.2016.07.025.
15. Heidari-Rarani, M., Rafiee-Afarani, M., Zahedi, A. M. (2019). Mechanical characterization of FDM 3D printing of continuous carbon fiber reinforced PLA composites. *Composites Part B: Engineering, 175,* 107147. DOI 10.1016/j.compositesb.2019.107147.
16. Dupont (2017). *Properties of Dupont Kevlar. Kevlar Aramid Fiber Technical Guide*. USA: Dupont.
17. The Thread Exchange (2019). *Kevlar thread guide*. The thread exchange. https://www.thethreadexchange.com/miva/merchant.mvc?Screen=CTGY&Category_Code=kevlar-thread-information.
18. Toray Carbon Fibers America Torayca T300 Data Sheet (2018). *Technical data sheet*. Toray Carbon Fibers America, Inc. https://toraycma.app.box.com/s/ru9sr1uzk0nw6vhilrt8hrmofytpjm1r.
19. Pal, S., Gandhi, R. (1988). Effect of twist on mechanical properties of twisted textured polyester yarn. *Indian Journal of Textile Research, 13,* 184–187.
20. Dickson, A. N., Barry, J. N., Mcdonnell, K. A., Dowling, D. P. (2017). Fabrication of continuous carbon, glass and Kevlar fibre reinforced polymer composites using additive manufacturing. *Additive Manufacturing, 16,* 146–152. DOI 10.1016/j.addma.2017.06.004.